Review Article

# Carbon Nanotube-Gold Nanoparticle Conjugates: An Advance Technology in Biomedical Field

A. TYAGI, S. BOSE*, V. MISHRA, T. KATARIA, G. KAUR, JASPREET, K. SINGHLA, PROMILA SHARMA[1] AND PRERNA UNIYAL[1]

Department of Pharmaceutical Sciences, Lovely Professional University, Jalandhar, Punjab 144401, [1]Graphic Era Deemed to be University, Dehradun, Uttarakhand 248002, India



**Nanoparticles (1-100 nm) provide several advantages, including lower toxicity, a relatively small dosage, and a high degree of manipulability, compared to conventional treatments. The use of nanoparticles for imaging and diagnostic purposes, as well as for drug and genetic delivery technologies, is of special interest to the biomedical industry. Liposomes, neosomes, micelles, gold nanoparticles, silver nanoparticles, carbon-based carriers such as carbon nanotubes and others are a few examples of the various forms of nanoparticles. Carbon nanotubes are widely used as drug carriers due to their good thermal and electrical conductivity, excellent sensitivity and high drug-loading capacity, while gold nanoparticles are popular for their biocompatibility, high surface modification potential and bioimaging properties. Due to the combination of their distinct features during conjugation, gold nanoparticles-carbon nanotubes conjugates have a wide range of applications. These conjugates are used in numerous biomedical fields as immunosensors, drug carriers, biosensors, electrochemical enhancers, bioimaging agents, nanoreactors, theranostics and more. The ability of gold nanoparticles to serve as bioimagers, combined with the extensive drug-carrying capacity of carbon nanotubes, has generated significant interest in gold nanoparticles-carbon nanotube conjugates for drug delivery and theranostic applications.**

**Key words: Carbon nanotube, gold nanoparticles, bioimaging, biomedical, drug carrier**

Nanotechnology is an advanced field that deals with materials and devices at sizes no larger than 100 nm[1]. Generally, Nanoparticles (NPs) are designed to fulfil two requirements; first, they must have a specific function, such as antibacterial activity or antitumor ability; and second, they must operate safely and target the intended site without harming normal tissue[2]. Effective drug targeting, reduced toxicity, prolonged drug release and increased half-life are key advantages of nano drug carriers[3]. Nanotechnology plays diverse roles in both biomedical fields and the food industry. It also contributes to the development, characterization, and modification of nanomaterials. These nanostructures enhance the *in vivo* solubility of food materials and drugs, thereby increasing their bioavailability. Additionally, nanomaterials enable controlled release and targeted drug delivery[4]. Fig. 1 represents the different types of materials used in nanotechnology.

## GOLD NANOPARTICLE (AuNP)

Nanostructures play an advanced role in nanomedicine across various fields, including drug delivery, nanoimaging, tissue engineering, antibacterial agents, nanomachinery and etc[5]. NPs possess specific physical, chemical and biological properties that serve as novel building blocks for the design of various medical diagnostic and therapeutic systems[6]. The nanoscale size and increased surface area of nanocarriers result in enhanced solubility and permeability of encapsulated molecules[7]. NPs offer several advantages over traditional treatments, including minimal toxicity, low effective dosage and a high degree of manipulability. They can be composed of a variety of organic or inorganic materials[8]. Inorganic nanomaterials such as AuNPs, show diversity with their improved optical, electrical, mechanical and thermal properties[9]. Gold nanomaterials of different sizes and shapes can be

***Address for correspondence**
E-mail: sjtbose308@gmail.com



**Accepted 24 December 2024**
**Revised 26 June 2024**
**Received 22 December 2023**
**Indian J Pharm Sci 2024;86(6):1935-1947**

synthesized using various preparation methods, as shown in fig. 2[10]. The specific characteristics of AuNPs enable numerous advanced biomedical applications, including bioimaging, gene delivery, enhanced contrast in X-ray computed tomography, tissue engineering, targeted drug delivery, as well as use as biosensors and theranostic agents[11]. AuNPs can be fabricated using various methods based on chemical, physical and biological processes, as shown in fig. 2.

## Properties:

AuNPs display remarkable features that distinguish them from metallic gold, highlighting their enormous potential for use in medicine. These features include outstanding optical and electronic properties, good mechanochemical stability, Surface Plasmon Resonance (SPR), special catalytic activity and ease of surface functionalization. Additionally, AuNPs exhibit excellent size dispersion, tunable shapes and resistance to oxidation[12]. In addition to its high density and atomic number of 79, gold has favorable X-ray attenuation properties[13]. These properties enable their use in mechanical and optical applications, as well as in catalytic, antibacterial and anticancer activities[14].

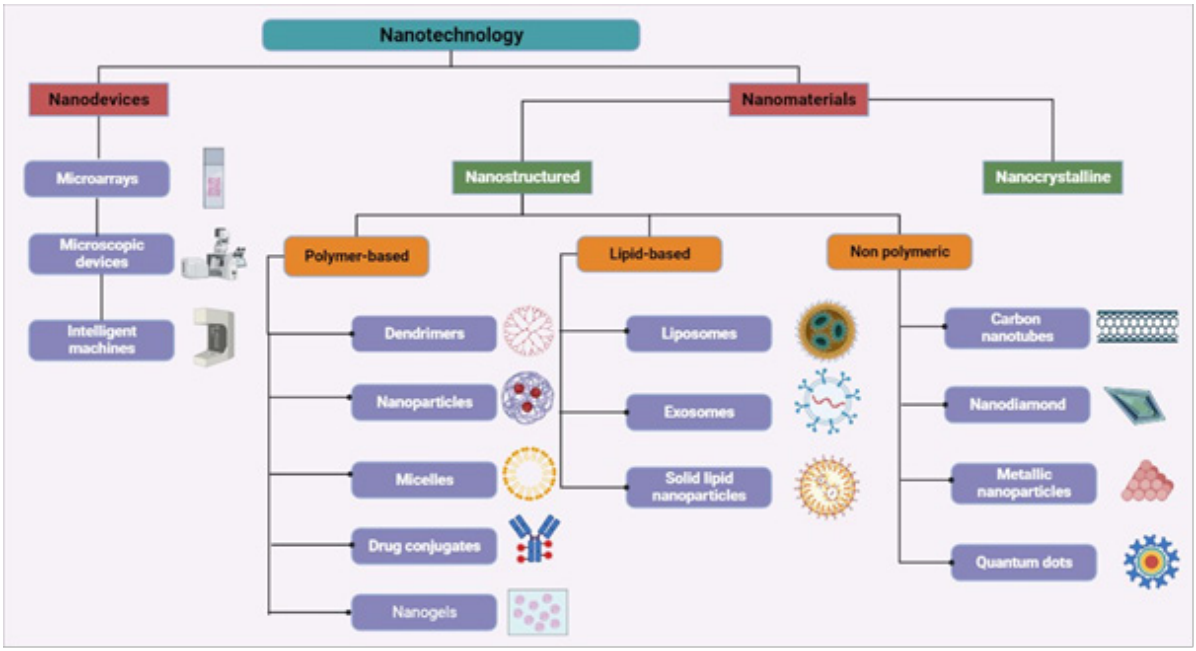


**Fig. 1: Nanotechnology in biomedical field**

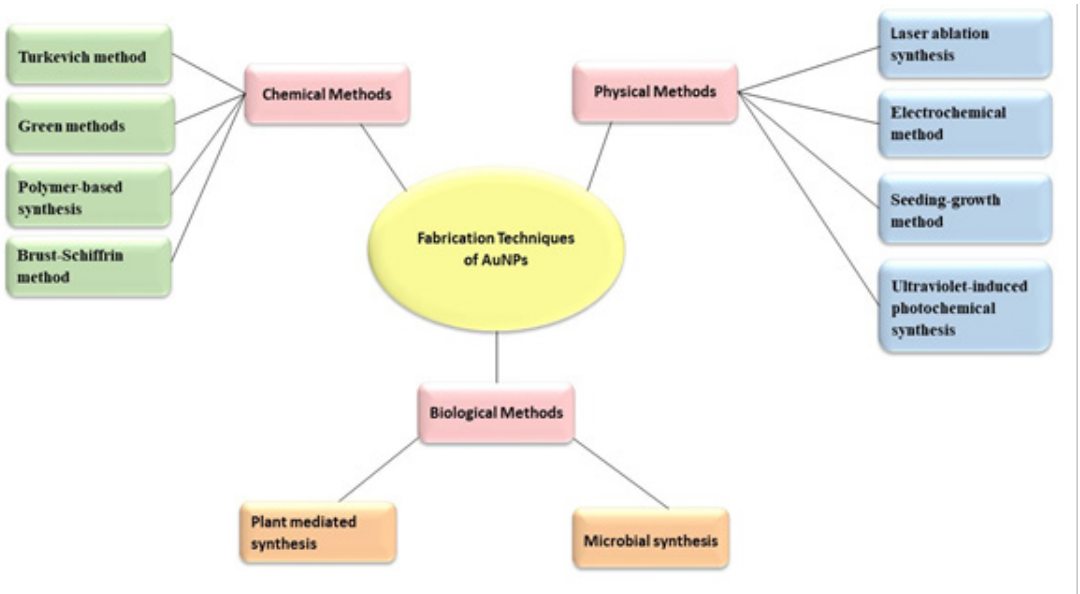


**Fig. 2: Fabrication of AuNPs**

## Carbon Nanotubes (CNTs):

CNTs are a renowned synthetic carbon allotrope. They differ from other nanocarriers due to their distinctive arrangement of carbon atoms, as well as their $sp^2$ hybridization, cylindrical structure with a C-C distance of 1.42 Å and an interlayer spacing of 3.4 Å. In addition, CNTs have been used for various delivery purposes, such as drug, gene and vaccine delivery, as well as in other biomedical applications due to their unique thermal, mechanical, electrical, optical and biological properties[15]. Due to the presence of several graphene layers, Multi-Walled CNTs (MWCNTs) and Double-Walled CNTs (DWCNTs) are mechanically stronger than Single Walled CNTs (SWCNTs), making them more useful in the field of composite materials[16]. Fig. 3 illustrates the classification of CNTs into four different types: SWCNTs, DWCNTs, MWCNTs, and Triple-Walled CNTs (TWCNTs).

## Fabrications of CNTs:

CNTs can be prepared by various methods, and the widely used methods for their fabrication are shown in fig. 4.

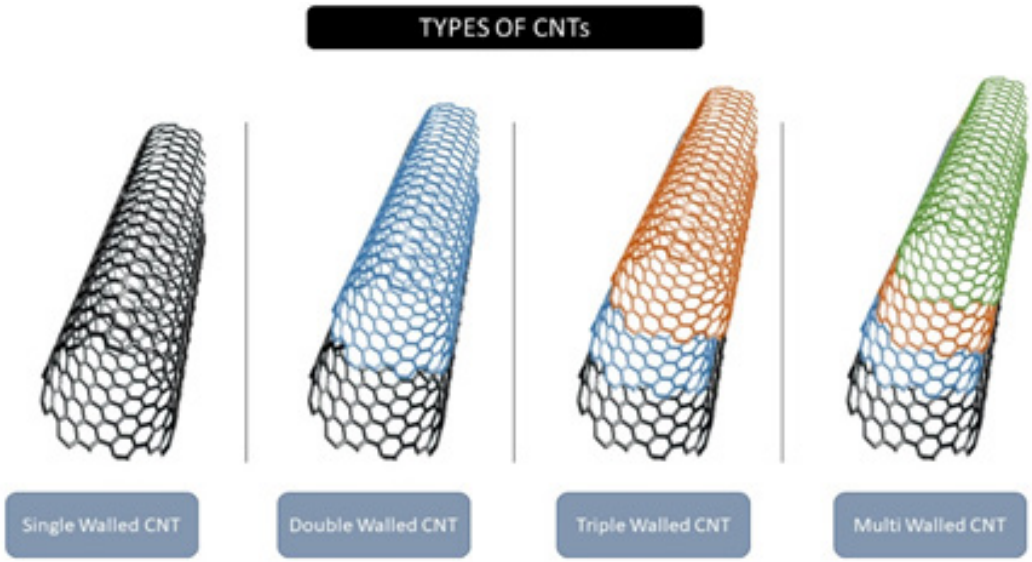


**Fig. 3: Classification of CNTs**

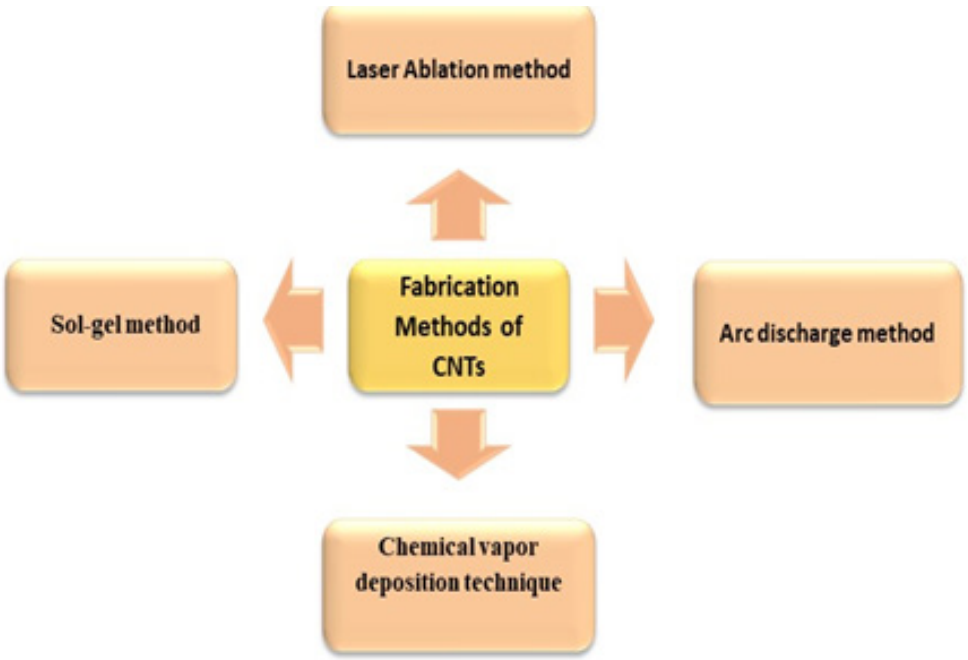


**Fig. 4: Fabrication techniques of CNTs**

**Properties of CNTs:**

Due to their huge surface area and exceptional mechanical, chemical and electrical capabilities, CNTs are frequently used as supporting electrode matrices in electrochemical biosensors[17]. A single CNT typically has an electrical conductivity in the range of $10^4$-$10^7$ $(\Omega\text{-m})^{-1}$. However, MWCNTs generally exhibit higher voltage, resulting in increased electrical conductivity. Additionally, since they are essentially rolled-up graphene sheets, MWCNTs share the extraordinary physical properties of graphene. Their tensile strength can reach up to 100 GPA, thermal conductivity is 3500 $Wm^{-1}K^{-1}$, electrical conductivity is $2\times10^7$ $(\Omega\text{-m})^{-1}$ and ampacity can reach up to 1013 A m-2[18]. Near-Infrared (NIR) photoluminescence is one of the intrinsic optical properties of CNTs, making them excellent bioimaging probes[19]. They possess numerous antibacterial and antifungal properties, function as protein transporters, contain exposed functional groups and exhibit rapid electron transfer kinetics. They are chemically inert, ultra-lightweight and more biocompatible than other materials. Additionally, they have semi-metallic conductive properties, making them ideal for a variety of applications, including environmental monitoring, clinical diagnostics and food safety[20].

## AuNPs AND CARBON NANOTUBE CONJUGATES

Yola *et al*.[21] synthesized AuNPs with average sizes of 20-22 nm using

Trisodium citrate ($Na_3C_6H_5O_7$). Dihydrogen monoxide ($OH_2$) as a reducing agent and

Chloroauric acid ($HAuCl_4$).$3H_2O$ as a precursor, in accordance with the literature. Following the preparation of a carboxylated MWCNT solution (0.1 mg/ml) in ethanol, the solution was kept in contact for 12 h with a solution of N-Hydroxysuccinimide (NHS) (50.0 mM, 10.0 ml) and dimethylaminopropyl carbodiimide (50.0 mM, 10.0 ml). The next step involved introducing the activated MWCNTs (at a 1:1 v/v ratio) into a solution of 4-Aminothiophenol (ATP) (1.0 mM), and a 2-hour self-assembly esterification process was carried out to produce thiol-functionalized MWCNTs (S-MWCNTs). A mixture of S-MWCNTs (0.2 mg/ml) and AuNPs (20.0 mg/ml) was then mixed for 20 min due to the sulfur-gold affinity. The resulting AuNP/S-MWCNT complex was then held at 25°.

Han *et al*.[22] used ion exchange chromatography to prepare CNTs, which were Deoxyribonucleic Acid (DNA)-coated into fractions based on various electronic configurations. The resulting DNA-CNTs were treated in a 0.2 M (N-Morpholino) Ethanesulfonic acid (MES) solution containing 4 mm EDC and 10 mm sulfo-NHS for 30 min at room temperature for activation. Next, CNT solution was mixed with amine@DNA at a concentration of 0.5 M. The mixture was then subjected to a 100 K centrifugal filter with configurations of 6000 rpm for 3 min to remove any unbound DNA after an overnight incubation at room temperature. To improve the fabrication of 3D radial CNT@AuNP nanoclusters, the DNA@end@functionalized CNTs and DNA@ modified@AuNPs were combined in a volume ratio of 1:4 and left to undergo a process from 50° to room temperature overnight.

Shi *et al*.[23] prepared AuNPs/Tetraamino Phenyl Porphyrin (TAPP)-functionalized MWCNTs (MWCNTs-CONH-TAPP) modified Glassy Carbon Electrodes (GCE) by combining AuNPs, MWCNTs-CONH-TAPP, and GCE. The GCE was polished with 0.05 µm alumina powder, followed by sonication in an ethanol/water mixture (1:1 ratio) and then rinsed with double-distilled water. The mixture was then dried under atmospheric $N_2$ at room temperature. Next, 2 mg of MWCNTs-CONH-TAPP was suspended in a Dimethylformamide (DMF) solution. The GCE surface was moistened with 6 µl of MWCNTs-CONH-TAPP preparation, followed by drying under infrared light for 10 min. Afterwards, the MWCNTs-CONH-TAPP/GCE was dipped into a 0.2 g/l chloroauric acid ($HAuCl_4$) solution and treated at a constant voltage of -0.2 V for 90 s. Finally, distilled water was used to rinse the AuNPs/MWCNTs-CONH-TAPP nanocomposite-modified GCE.

Chinh *et al*.[24] fabricated AuNP-CNT nanoconjugates by reducing gold ions with sodium citrate, which served as the basis for the creation of Au-CNT nanocomposites. An aqueous suspension of CNT (0.3 mg/ml) was mixed with an $HAuCl_4$ solution (0.01 M) to prepare the nanocomposites. The resulting mixture was sonicated for 30 min to enhance the interaction between AuNPs and CNTs. Then, a 2 % sodium citrate solution was added to the AuNP-CNT suspension, which was heated to 90°. The mixture was maintained under these conditions for 1 h. The resulting nanocomposite was centrifuged and rinsed with distilled water at 12 000 rpm. Finally, the nanocomposite was dried overnight at 80°[24].

Wang *et al*.[25] synthesized magnetic MWCNT-AuNP composites by mixing $FeCl_3.6H_2O$ (0.14 g) and

MWCNT (0.04 g) with a gold solution in a glass vial containing 7.5 ml of ethylene glycol, followed by the addition of 0.36 g of sodium acetate. The mixture was stirred for 30 min at room temperature using a magnetic stirrer. After thorough mixing, the solution was transferred to a stainless-steel reactor with a Teflon coating and heated at 180° for 8 h. Once the reaction was complete and the mixture had cooled to room temperature, it was rinsed 5 times with water. A magnet was then placed at the bottom of the beaker to collect the magnetic material, which was subsequently dried at 80° to obtain the MWCNT-AuNP hybrid material.

AuNP-CNT conjugates can be synthesized using various methods depending on the requirements, and the conjugated product is obtained, as shown in fig. 5.

## BIOMEDICAL APPLICATION OF AuNP-CNT CONJUGATES

### Immunosensor:

Huang *et al*.[26] fabricated an Au-PEI-CNT immunosensor, which showed an effective linear response to Aflatoxin B1 (AFB1) concentrations in a broad range from 0.05 to 25 ng/ml. This sensor incorporated AuNPs into the CNTs with Polyethyleneimine (PEI) in a soft, linear arrangement. In contrast to an Au-PEI-CNFs-based sensor, the detection limit was found to be 0.093 ng/ml. The proposed immunosensor exhibited excellent selectivity, reproducibility, and storage stability. The fabricated immunosensor can be used for the analysis of wheat samples with a high level of sensitivity and reliability.

Valverde *et al*.[27] fabricated an immunosensor using a hybrid nanomaterial composed of MWCNTs and AuNPs as nanocarriers for the detection of multiple antibodies and Horseradish Peroxidase (HRP) molecules. The proposed immunosensor was employed to identify the Receptor activator of Nuclear Factor kappa-B (NF-κB) ligand (RANKL) in the serum of patients with rheumatoid arthritis or colorectal cancer. 5 l of undiluted serum were used in each test, with detection taking less than 2 h, including the time required to prepare the blocked samples. This work provides a clear description of the first integrated electrochemical immunosensor for detecting RANKL, a biomarker critical for regulating bone resorption and influencing immune system responses, which may contribute to tumor growth and metastasis during cancer progression. The RANKL linear calibration plot ranged from 10.4 to 1,000 pg/ml, with a Limit of Detection (LOD) of 3.1 pg/ml, achieved through amphoteric detection using hydrogen peroxide or hydroquinone.

Takemura *et al*.[28] used AuNPs, magnetic NPs, and CNTs to achieve magnetic separation from interference and signal amplification using a nanocomposite of the virus. AuNPs exhibit SPR, while Quantum Dots (QDs) show a viral fluorescence enhancement effect based on concentration when the target virus is present. To facilitate target binding in a sandwich format, both nanomaterials were coupled with antibodies specific to influenza virus A. Additionally, the immunosensor was able to detect the virus even in a human serum matrix, relying on these two signals during viral detection. For optical detection, the LOD was found to be fg/ml, whereas for electrochemical detection, the LOD was 13.66 fg/ml[28].

Adabi *et al*.[29] developed an electrochemical-based immunosensor for the detection of epidermal growth factor receptor 2 in humans, utilizing an electrospun carbon nanofiber. The proposed immunosensor showed a linear response range of up to 5-80 ng/ml, with a detection limit of 0.45 ng/ml. Due to its non-invasive, accurate and rapid analysis characteristics, the immunosensor demonstrated high potential for determining the target.

Tao *et al*.[30] developed an ultrasensitive PDG/AuNPs/MWCNTs/rGO immunosensor to detect Alpha (α)-Synuclein Oligomers (syno), which serve as an early biomarker in Parkinson's disease. The PDG/AuNPs/MWCNTs/rGO complex nanocomposite is mounted on the surface of a GCE to function as the signal amplification material before being grafted with anti-syno antibodies, which precisely identify and bind with syno. Using Square Wave Voltammetry (SWV), the proposed immunosensor showed a linear response between 0.05 fM and 500.00 fM, with a detection limit of 0.03 fM. The immunosensor's excellent sensitivity, specificity and stability were demonstrated in the analysis of syno in human plasma samples.

Peng *et al*.[31] developed an indirect Enhanced Chemiluminescence (ECL)-based immunosensor for the highly sensitive quantification of osteoarthritis (OA), benefiting from multiple amplification steps. The immunosensor exhibited an optimum half-maximal inhibitory concentration (IC50) of 0.25 ng/ml, a linear range of 0.01-20 ng/ml and a low detection limit of 0.005 ng/ml. Additionally, the proposed ECL immunosensor was successfully applied to detect OA in mussel samples. This work advances the use of

codoped Graphene QDs (GQDs) in the development of ECL-based immunosensors for the detection of shellfish toxins and contributes to the progress of ECL-based luminophores.

Liu *et al*.[32] developed an immunoassay in which AFB1@Streptavidin (AFB1@SA) conjugates were used to bind with the Head Count Ratio(HCR), a biotinylated double-stranded DNA (dsDNA) in nanostructured form, for amplification, signal reporting and as a competitor. An anti-AFB1 antibody with smaller molecular size was densely coated on the surface of (AuNPs/WS2/MWCNTs). The proposed immunosensor showed a good linear correlation (0.5-10 ng/ml) with AFB1 under optimal conditions, with a sensitivity of 2.7 A ng/ml and an extremely low detection limit of 68 fg/ml. Specificity tests demonstrated that the immunosensor exhibited no apparent cross-reactivity with Ochratoxin A (OTA), Deoxynivalenol (DON), Zearalenone (ZEN), or Fumonisin B1 (FB1).

Wang *et al*.[33] developed an immunosensor for measuring Interleukin-6 (IL-6). The antibody was directionally captured by Staphylococcal Protein A (SPA) to reduce steric hindrance caused by random immobilization. The immunosensor demonstrated satisfactory performance for IL-6 detection due to the effective immobilization of the IL-6 antibody on the sensing surface *via* SPA. Under optimal conditions, the biosensor showed a LOD of 2.87 pg/ml and a linearity range in blood samples from 0.01 ng/ml to 800 ng/ml. Additionally, the sensor accurately measured IL-6 levels in blood and other tissue fluids (liver, heart and lung) from rats that had suffered a myocardial infarction. The success of the proposed sensor not only expands its potential for clinical IL-6 monitoring but also provides a novel approach for studying inflammation in rats.

He *et al*.[34] developed a sensitive and specific immunoassay with dual signal readouts to detect Microcystin-LR (MC-LR). First, the microplate was modified with CNTs adorned with AuNPs (AuNP-CNTs) to encapsulate enough antigens, using the excellent affinity of AuNPs and the high surface area of CNTs. Then, gold nanorods were coated with silver nanoparticles to create a composite material that resembled maize, which was used to collect secondary antibodies and initiator DNA strands. The current responses of silver and copper ions were read out using differential pulse stripping voltammetry and acid treatment to provide a dual-signal readout. The detection limit of 2.8 ng/l was found to be lower compared to other methods. MC-LR could be detected using a competitive immunoreaction in a linear range from 0.005 µg/l to 20 µg/l.

Hu *et al*.[35] utilized the NPs MWCNTs@AuNPs to build the sensing platform. These NPs provided a matrix that was highly efficient for immobilizing a significant number of coating antigens and also facilitated the amplification of electronic transmission, enhancing the intensity of ECL. The sensor demonstrated excellent characteristics such as sensitivity, stability, and a broad linear range for detection. The range of 2′7′-Dichlorofluorescein (DCF) was found to be 0.005 ng/ml to 1000 ng/ml, with a detection limit of 1.7 pg/ml, based on the amplified effect of GO/g/$C_3N_4$ and the MWCNTs@AuNPs nanocomposite. Additionally, the sensor was applied to actual samples, yielding positive results. Thus, the proposed work offers a potential technique for DCF detection and for detecting other small substances in the future.

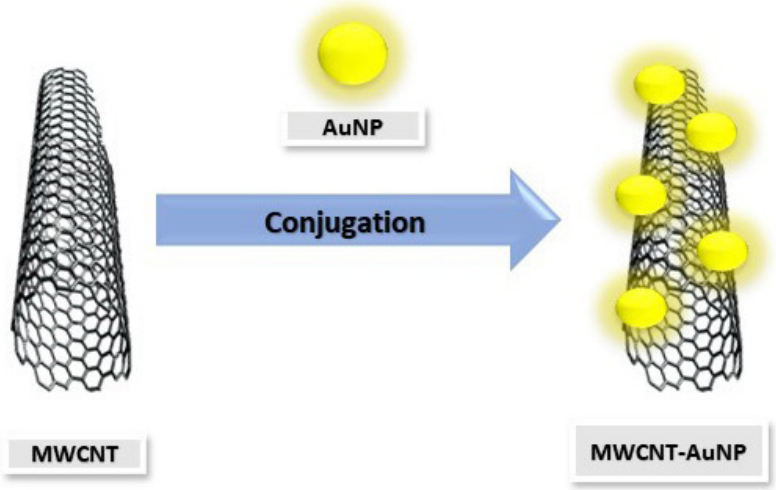


**Fig. 5: CNT and AuNP conjugates**

**Biosensor:**

Peng *et al*.[36] fabricated a biosensor consisting of recombinant Human Erythropoietin (rHuEpo) in its reduced form (rhuEPO)@AuNPs@CNT, a nanocomposite modified with a GCE. The selectivity of the biosensor was enhanced by the reduced rhuEPO. Additionally, amperometric tests showed a linear range of 0 to 22 000 ng/l and a sensitivity of 4.390 µA/(gl) for the rhuEPO@AuNPs@CNTs@GCE toward rHuEpo. The biosensor could be used to determine rhuEPO levels in blood samples from cyclists. Chen *et al*.[37] fabricated a biosensor that demonstrated the popular diagnostic marker known as SPR biosensing for human cardiac Troponin I (cTnI), which is associated with myocardial injury, utilizing immunomagnetic separation technology. A secondary Antibody (Ab2) conjugated to multi-walled carbon nanotube-Polydopamine (PDA)-AgNPs (MWCNTs@PDA@AgNPs@Ab2) was incorporated into the sensing system, where it occupies the remaining binding sites of cTnI, thereby enhancing the SPR response signals. The detection limit for cTnI was found to be 3.75 ng/ml, which is 320 times lower than that achieved using a PDA-based sensing technique. The assessment of blood samples spiked with cTnI was conducted using this technology, and the successful recoveries suggest that it could be useful for clinical diagnosis in the future.

Maity *et al*.[38] developed an innovative biosensor using a Screen-Printed Carbon Electrode (SPCE) functionalized with amine-ended multiwalled CNTs, polyaniline, reduced graphene oxide and AuNPs. With the help of GOx, the highly sensitive glucose biosensor was immobilized on the SPCE. Compared to the bare SPCE, the modified SPCE increased the current by 13.43 times at the minimum operating potential. The glucose biosensor exhibited excellent reproducibility (90.23 %, n=7), high stability (96 % after 30 d of storage at 20°, and 74.5 % after 2 w at 4°), a broad linear range 1-10 mm, a low Kmapp value (0.734), a minimum detection limit (64 nm), and high sensitivity (246 µA/mM/mm$^2$). An amperometric approach was used to validate the biosensor in human blood serum samples for glucose level determination. As expected, the SPCE-based nanocomposite platform proved to be an effective glucose sensor, offering a foundation for various biochemical sensors. Wu *et al*.[39] produced a biosensor consisting of $Ti_3C_2$-MXene@AuNPs composites conjugated with MWCNTs-PDA-AgNPs-polyclonal anti-CEA antibody (MWPAg-$Ab_2$) in a sandwich format, offering a wide range for CEA determination. The demonstrated biosensing strategy exhibited excellent sensitivity and strong repeatability for detecting CEA in actual serum samples, making it a viable tool for cancer screening and quick detection of CEA in human serum.

Zhang *et al*.[40] fabricated an highly effective electrochemical biosensing system, L/D-DHCNT-PPy-AuNP-L/D-Cys, which exhibited enhanced sensitivity and conductivity. Additionally, the system demonstrated chiral recognition of amino acids such as tyrosine, tryptophan and glutamic acid, showing its capacity to recognize amino acid enantiomers chirally. This opens up new possibilities for its potential use in chiral biosensors. Rabai *et al*.[41] proposed a biosensor that demonstrated excellent performance for cadmium detection at a low applied voltage (0.5 v), achieving a maximum sensitivity of 1.2 km$^{-1}$. The aptasensor also showed maximum selectivity against interfering ions such as $Pb^{2+}$, $Hg^{2+}$ and $Zn^{2+}$. This electrochemical biosensor offers an easy-to-use and accurate method for detecting $Cd^{2+}$ in aqueous solutions, with potential applications in monitoring trace metal concentrations in real-world samples.

Hu *et al*.[42] observed that the presence of developing polymer segments with the opposite charge facilitated the accumulation of carbon nanotubes. AuNPs/MWCNT-Poly(3,4-Ethylenedioxythiophene) (PEDOT) was synthesized in aqueous conditions. In the MWCNT-PEDOT film, AuNPs were electrochemically deposited in highly conductive microporous spaces. The resulting hybrid coating exhibited excellent conductivity, fast electron transport (a 3.5-fold increase) and high porosity. This study provides an excellent electrochemical transducing scaffold for deactivating acetylcholinesterase with high affinity (Kappm=0.182 mM), offering potential for further applications in monitoring neurodegenerative disorders. Du *et al*.[43] designed an electrochemical biosensor to detect the modification of E-cadherin and examine various stages of Epithelial-to-Mesenchymal Transition (EMT) by utilizing the exceptional performance of QD-nanocomposite materials. Additionally, differential pulse voltammetry revealed a synergistic interaction between carbon nanotube-AuNPs and QDs, which enhanced the electrochemical signals, making them responsive and sensitive. Thus, our research demonstrated that electrochemical sensing is a reliable tool for identifying EMT and may have several applications in studying different cell type transitions.

Wang *et al*.[44] developed a CNTs (MWCNTs)-stabilized

Au cluster complex using N-Acetyl-L-Cysteine (NAC). The complex-modified GCE was fabricated and used for electrochemical sensing applications as a novel working electrode by drop-casting the complex onto the GCE surface. The minimum detection limits were 30 nm for dopamine and 40 nm for uric acid, with linear detection ranges of 0.1-250 µm and 0.1-300 µm, respectively. The complex-modified GCE demonstrated excellent performance for the selective detection of dopamine and uric acid in actual human blood and urine samples, with detection recoveries ranging from 96.9 % to 104.7 % and a low relative standard deviation of 1.1 % to 3.7 %. Zhang *et al*.[45] proposed a biosensor modified with GCE and functionalized with 3,4,9,10-Perylene Tetracarboxylic Acid (PTCA), MWCNTs, and AuNPs (PTCA@rGO@MWCNT@AuNP@GCE). Additionally, the fabricated biosensor exhibited high sensitivity and selectivity for the detection of dopamine in actual samples. Ibrahim *et al*.[46] proposed a sensor using Glassy Carbon Paste (GCP) as a crosslinker to produce carboxylated MWCNTs-COOH, which were then coated with AuNPs. The modified biosensor exhibited a cathodic response towards Corrosion Prevention Association (CPA), resulting in a significant increase in the threshold current (42 µA) compared to the unmodified sensor with GCPE (4 µA). Additionally, it demonstrated high sensitivity, good reproducibility, and long-term stability, making it suitable for measuring CPA in pharmaceutical products (such as androcur), as well as in urine samples and human blood serum.

Inagaki *et al*.[47] developed nanocomposite films with Polythiophene (PT), AuNPs, and CNTs. The incorporation of CNTs enhanced the stability of the films electrochemically, compared to equivalent films without CNTs. The potential of the produced nanocomposite as an electrochemical sensor for dopamine voltammetry was assessed. The PT/Au/CNT film, which took 4.5 h of processing to produce, yielded the best results, with a low detection limit of 0.69 µmol/l. Salvo-Comino *et al*.[48] fabricated an effective, simple and biocompatible biosensor for the detection of catechol. Additionally, a polymeric matrix of chitosan was encapsulated in an AuNP/CNT nanocomposite, which was then accumulated on the surface of boron-doped diamond. The proposed biosensor exhibited good affinity for detecting catechol in red wine sample.

Zhang *et al*.[49] proposed an N-doped CNTs-$Fe_3O_4$-Au nanocomposite that facilitated the immobilization of cytochrome c, which contributed to the development of biosensors with high sensitivity. The cyt c-NCNTs-$Fe_3O_4$-Au nanocomposite exhibited a low detection limit of 0.3 µm for $H_2O_2$ detection, demonstrating the potential of the proposed biosensor for the development of novel biosensors. This biosensor could overcome most electrochemical interferences, leading to increased sensitivity. Lotfi *et al*.[50] developed a direct and rapid method for the determination of T4 using MWCNTs/CC-SH/Au on a GCE. The fabricated sensor offered several advantages, including quick preparation, low cost, high stability and excellent reproducibility. Additionally, the conjugation of the MWCNTs@CC-SH@Au nanocomposite with the GCE served as a modifier, enhancing electron transfer kinetics, surface area and electrocatalytic activity. The sensor demonstrated outstanding electroanalytical performance, exhibiting good linearity, reproducibility, and sensitivity, along with a low detection limit. The proposed biosensor could be used for detecting T4 in human blood samples, with results, validated by High Performance Liquid Chromatography (HPLC).

**Aptasensor:**

Lu *et al*.[51] proposed a CEA Aptamer-based aptasensor in which an Au/CNT cathodic substrate was used to facilitate target identification. This process depended on a clear decrease in the current signal caused by the halted amplification of the BOD labels and the steric hindrance of the captured CEA molecules. The PEC biosensing system, consisting of a two-electrode setup, exhibited excellent sensitivity, with a photoanode made of ZIS/Fe-$TiO_2$ and the outstanding oxygen-reduction ability of the BOD labels. The two-electrode PEC biosensing system demonstrated remarkable sensitivity, attributed to the superior PEC features of the ZIS@Fe-$TiO_2$ photoanode and the excellent oxygen-reduction capability of the BOD labels. The platform also showed selectivity in a biological matrix due to the partitioning of biorecognition with the photoanode. This sophisticated two-electrode approach offers a promising route for developing reliable PEC biosensors for use in complex biological samples.

Azadbakht *et al*.[52] determined kanamycin using an impedimetric technique based on aptamers. Molybdenum Selenide ($MoSe_2$) nanoflowers, which are attractive materials for sensing due to their high specific surface area and excellent electrical conductivity, were synthesized using a hydrothermal method. AuNPs and $MoSe_2$ nanoflowers (AuNP/CNT/$MoSe_2$) were then added, and CNTs were deposited onto a GCE to serve as a signal amplifier. Electrochemical Impedance

Spectroscopy (EIS) was used to measure variations in the electrochemical signal. The calibration plot revealed a detection limit of 0.28 pM, and linearity was observed for kanamycin concentrations ranging from 1 pM to 0.1 nM and 100 nM to 10 µm. He *et al*.[53] developed a disposable and portable aptasensor using AuNPs/carboxylated MWCNTs (cMWCNTs) coupled with a Thionine (Thi)-modified complementary strand of aptamer copy DNA (cDNA). The bioconjugate (AuNPs/MWCNTs/cDNA@Thi) was released by Thin-Film Gold Electrodes (TFGEs) for the rapid and sensitive detection of Oxytetracycline (OTC). As a result, the electrochemical signal dropped significantly. The aptasensor demonstrated excellent stability, good selectivity and high sensitivity. Additionally, the TFGE-based electrochemical aptasensor exhibited a large dynamic range (1013-105 g/ml) for OTC, with a low detection limit of $3.1\times10^{14}$ g/ml. The proposed aptasensor showed effective results in detecting OTC in chicken samples.

Liu *et al*.[54] synthesized an AuNP-Thi-CNTs nanocomposite by coating Thi-MWCNTs with AuNPs, which were approximately 3 nm in size. The nanocomposite was used to create a radiometric electrochemical aptasensor for 17-Estradiol (E2) by attaching it to an electrode and employing it as a redox-active signaling interface. The aptamer against E2 functions both as a collector and separator, specifically binding to E2. In the concentration range of 12 pm to 60 nm, the electrode displayed two peak signals:one that increased at +0.50 V *vs*. SCE for E2 and another that decreased at 0.32 V for Thi. The current ratio can thus be used to measure the concentration of E2 accurately, consistently and sensitively.

**Drug carrier:**

Anirudhan *et al*.[55] proposed a drug carrier system in which Diclofenac Sodium (DS) was used as the model drug. In this system, an AuNP/CNT nanocomposite was incorporated into a skin adhesive matrix containing polyvinyl alcohol@poly(dimethylsiloxane)-g-polyacrylate, which was used to create an electro-sensitive patch. The matrix was designed to improve electrical conductivity and skin permeability. The ability to fine-tune the device characteristics was achieved by varying the thermomechanical properties. Additionally, variations were made in the Water Vapor Permeability (WVP), drug release profile and encapsulation efficiency of the drug. The membrane with the highest Drug Encapsulation Efficiency (DEE) and thermomechanical characteristics was made with 1.5 % AuNP-CNT. The Transdermal Release Dynamics (TRD) of DS were investigated using rat skin with different AuNP/CNT concentrations and various voltage settings. The addition of AuNP-CNT enhanced the permeation profile of DS at an applied voltage of 10 V, with 1.5 % nanofibers performing the best. The barrier of the stratum corneum was effectively disrupted by electroporation in combination with AuNPs through various processes, including the destruction of the multilamellar lipid system, the creation of new aqueous passageways and heat action. Karthika *et al*.[56] aimed to enhance the biocompatibility for the delivery of Doxorubicin (DOX). The results showed that MWCNT was well-coated with $TiO_2$ and AuNPs. Hemolytic and antibacterial experiments demonstrated that the NDC had well-tuned biocompatible characteristics. The antioxidant potential of Nanocomposite Drug Carrier (NDC) was reported to be quite strong, at 80.7 % in terms of ascorbic acid equivalents. Commercially, DOX is used for the treatment of A549 and MCF7 cells, and its efficacy was significantly enhanced with the addition of NDC, which delivered the drug specifically at a pH of 5.5, with a loading capacity of 0.45 mg/ml. The drug release capacity was found to be 90.66 % over 10 h, a value that substantially exceeds most recent studies in the literature.

**Bioimaging:**

Qin *et al*.[57] developed SWCNT/Ag/AuNPs nanoparticles composed of an Ag/Au alloy. Under hypoxic conditions, the pre-assembled azobenzene was gradually removed from the SWCNT-Ag-AuNPs surface using various reductases, leading to the disappearance of the alkyne Raman band at 2,207 $cm^{-1}$. The detection proved to be effective in several cell lines as well as in tissue samples from rat livers obtained after hepatic ischemia surgery. The hypoxia levels were determined by the ratio of intensities of two peaks ($I_{2578}/I_{2227}$) in the SWCNT band range, with the 2578 $cm^{-1}$ band serving as the internal standard. Saghatchi *et al*.[58] demonstrated the effectiveness of functionalized MWCNTs with magnetic $Fe_3O_4$, conjugated with AuNPs, for bioimaging and cancer treatment. The MCF7 cell line was used to study radiation and thermotherapy *in vitro*. When employed as a contrast agent in ultrasound, CT and MRI imaging, mf-MWCNT/AuNPs showed significant advantages. They also absorbed radio waves and X-rays, enhancing the effectiveness of radiation and thermotherapy in killing cancer cells. Due to their beneficial properties in radio, thermo, and imaging treatments, mf-MWCNT/

AuNPs proved to be a promising multimodal tool for cancer therapy.

**Electrochemical enhancer:**

Wroblewska *et al*.[59] established cross-correlations between statistical data and the 2D and G mode characteristics, which allowed for a clear distinction between doping and strain. Additionally, the optical characteristics of the films were investigated. The effectiveness of CNT Raman scattering was enhanced by AuNPs. Resonance Raman spectroscopy on radial breathing modes showed that the enhancement was wavelength-dependent. The maximum enhancement factor was 1.7 eV, with a range of 2 to 3.5 times. The 5$^{th}$ order perturbation theory, including the plasmonic effect, was used to understand the geometries of the enhanced resonance Raman profiles. Cho *et al*.[60] found that the PS@t-CNT@AuNP exhibited effective topologies that reduced contact resistance by CNTs through AuNPs, as demonstrated by morphological analysis of the self-assembled structure. When comparing our manufacturing approach to the traditional electroplating method for creating conductive microspheres, it proved to be simpler, more affordable and biodegradable. The combination of Zero-Dimensional (0D) and One-Dimensional (1D) conductive fillers was found to be a valuable technique for achieving better conduction at lower filler concentrations, thereby reducing production costs and optimizing the efficiency of our manufacturing strategy.

**Nanoreactors:**

Li *et al*.[61] fabricated Polyethylene Glycol (PEG)-b@ Polyacrylic Acid (PAA)-Butyl Acrylate (BA)@X-PS-based PEG surface brushes, which were found to effectively prevent the aggregation of CNT@X-PS@ Au. Additionally, the required partitioning of the Au precursor and the growth of the Au shell were enabled by the intermediate PAA compartments, while the stability of the CNTs was maintained by the crosslinked X-PS blocks, preserving the inherent characteristics of the CNTs. The PEG-capped CNT@X-PS@Au nanocomposites were found to be recyclable and catalytically active. The various roles of AuNP-CNT conjugates have been discussed in fig. 6.

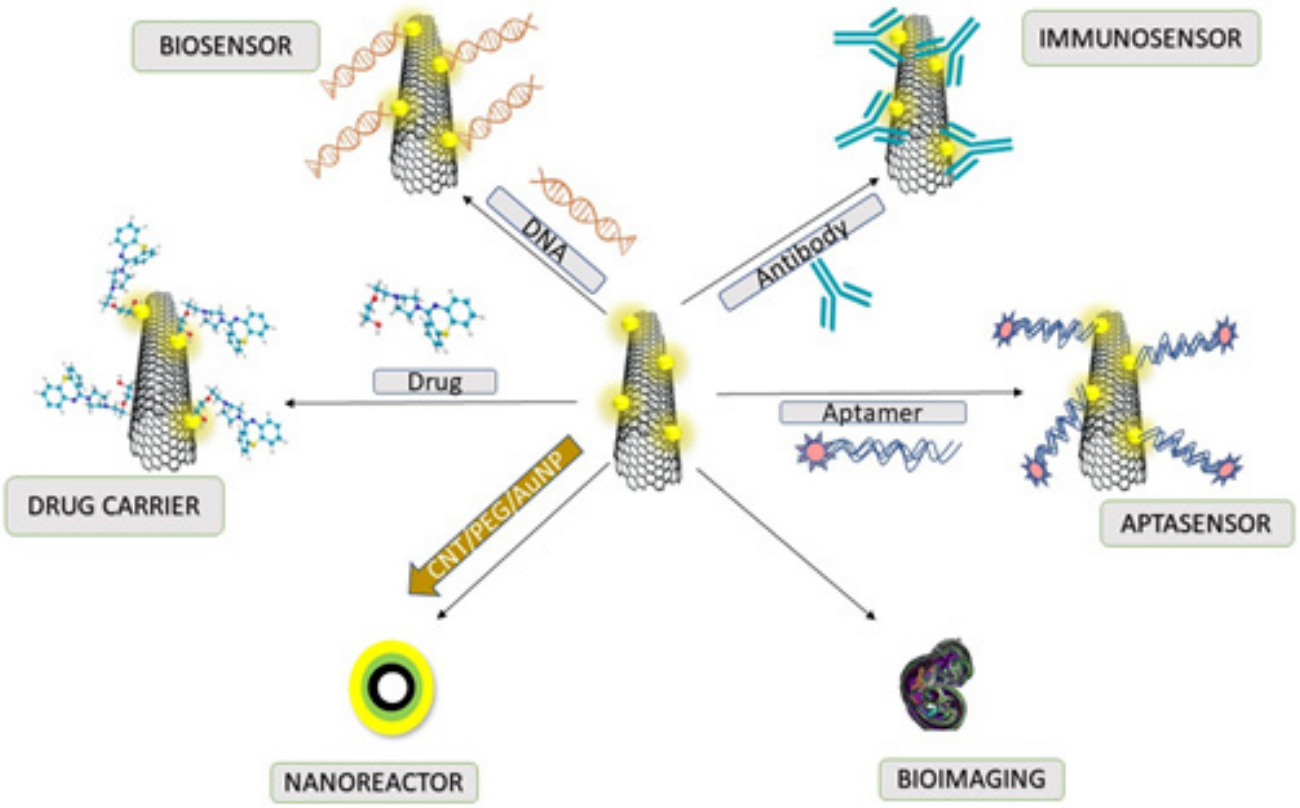


**Fig. 5: CNT and AuNP conjugates**

## CONCLUSION

The CNTs are insoluble in the majority of solvents. Therefore, their solubility can be enhanced through functionalization. Functionalized CNTs are more biocompatible compared to non-functionalized CNTs. Biosensors created with functionalized CNTs are highly sensitive, more stable, exhibit faster response times and can detect a wide range of analytes. Gold nanomaterial composites with MWCNTs serve as excellent biosensors due to the superior conductivity of MWCNTs and the easy surface modification of AuNPs. Copper-gold bimetallic nanocrystals incorporated into carbon nanotubes act as a unique tool for the sensitive detection of carcinoembryonic antigen, an emerging biomarker for various cancer diseases. Despite the unique properties of AuNPs and CNTs, they each have distinct limitations. To overcome these limitations and combine their properties to enhance biomedical applications, functionalized conjugates are of particular interest for drug delivery, theranostics and many other purposes.

### Conflict of interests:

The authors declared no conflict of interests.

## REFERENCES


1. Giakoumettis D, Sgouros S. Nanotechnology in neurosurgery: A systematic review. Childs Nerv Syst 2021;37:1045-54.
2. Wang Y, Zhang P, Wei Y, Shen K, Xiao L, Miron RJ, *et al*. Cell-membrane-display nanotechnology. Adv Healthc Mater 2021;10(1):2001014.
3. Klochkov SG, Neganova ME, Nikolenko VN, Chen K, Somasundaram SG, Kirkland CE, *et al*. Implications of nanotechnology for the treatment of cancer: Recent advances. Semin Cancer Biol 2021;69(1):190-9.
4. Sahani S, Sharma YC. Advancements in applications of nanotechnology in global food industry. Food Chem 2021;342:128318.
5. Damodharan J. Nanomaterials in medicine-An overview. Mater Today Proceedings 2021;37:383-5.
6. Sindhwani S, Chan WC. Nanotechnology for modern medicine: Next step towards clinical translation. J Intern Med 2021;290(3):486-98.
7. Saka R, Chella N. Nanotechnology for delivery of natural therapeutic substances: A review. Environ Chem Lett 2021;19(2):1097-106.
8. Yao CG, Martins PN. Nanotechnology applications in transplantation medicine. Transplantation 2020;104(4):682-93.
9. Sani A, Cao C, Cui D. Toxicity of Gold Nanoparticles (AuNPs): A review. Biochem Biophys Rep 2021;26:100991.
10. Zhang J, Mou L, Jiang X. Surface chemistry of gold nanoparticles for health-related applications. Chem Sci 2020;11(4):923-36.
11. Bansal SA, Kumar V, Karimi J, Singh AP, Kumar S. Role of gold nanoparticles in advanced biomedical applications. Nanoscale Adv 2020;2(9):3764-87.
12. Shedbalkar U, Singh R, Wadhwani S, Gaidhani S, Chopade BA. Microbial synthesis of gold nanoparticles: Current status and future prospects. Adv Colloid Interface Sci 2014;209:40-8.
13. Dong YC, Hajfathalian M, Maidment PS, Hsu JC, Naha PC, Si-Mohamed S, *et al*. Effect of gold nanoparticle size on their properties as contrast agents for computed tomography. Sci Rep 2019;9(1):14912.
14. Usman AI, Aziz AA, Noqta OA. Application of green synthesis of gold nanoparticles: A review. J Teknol 2019;81(1):171-82.
15. Prajapati SK, Malaiya A, Kesharwani P, Soni D, Jain A. Biomedical applications and toxicities of carbon nanotubes. Drug Chem Toxicol 2022;45(1):435-50.
16. Arunkumar T, Karthikeyan R, Ram SR, Viswanathan K, Anish M. Synthesis and characterisation of Multi-Walled Carbon Nanotubes (MWCNTs). Int J Ambient Energy 2020;41(4):452-6.
17. He L, Huang R, Xiao P, Liu Y, Jin L, Liu H, *et al*. Current signal amplification strategies in aptamer-based electrochemical biosensor: A review. Chin Chem Lett 2021;32(5):1593-602.
18. Zhang X, Lu W, Zhou G, Li Q. Understanding the mechanical and conductive properties of carbon nanotube fibers for smart electronics. Adv Mater 2020;32(5):1902028.
19. Raphey VR, Henna TK, Nivitha KP, Mufeedha P, Sabu C, Pramod KJ. Advanced biomedical applications of carbon nanotube. Mater Sci Eng C Mater Biol Appl 2019;100:616-30.
20. Anzar N, Hasan R, Tyagi M, Yadav N, Narang J. Carbon nanotube-A review on synthesis, properties and plethora of applications in the field of biomedical science. Sens Int 2020;1:100003.
21. Yola ML, Atar N. Novel voltammetric Tumor Necrosis Factor-Alpha (TNF-α) immunosensor based on gold nanoparticles involved in thiol-functionalized multi-walled carbon nanotubes and bimetallic Ni/Cu-MOFs. Anal Bioanal Chem 2021;413:2481-92.
22. Han S, Liu W, Zheng M, Wang R. Label-free and ultrasensitive electrochemical DNA biosensor based on urchinlike carbon nanotube-gold nanoparticle nanoclusters. Anal Chem 2020;92(7):4780-7.
23. Shi P, Xue R, Wei Y, Lei X, Ai J, Wang T, *et al*. Gold nanoparticles/tetraaminophenyl porphyrin functionalized multiwalled carbon nanotubes nanocomposites modified glassy carbon electrode for the simultaneous determination of p-acetaminophen and p-aminophenol. Arab J Chem 2020;13(1):1040-51.
24. Chinh VD, Hung LX, di Palma L, Hanh VT, Vilardi G. Effect of carbon nanotubes and carbon nanotubes/gold nanoparticles composite on the photocatalytic activity of $TiO_2$ and $TiO_2$-$SiO_2$. Chem Eng Technol 2019;42(2):308-15.
25. Wang Q, Wu X, Zhang Y, Hu M, Chen J, Gao J, *et al*. Preparation of a magnetic multiwalled carbon nanotube-gold nanoparticle hybrid material for the efficient extraction of triazine herbicides from rice. Anal Lett 2020;53(11):1740-56.
26. Huang Y, Zhu F, Guan J, Wei W, Zou L. Label-free amperometric immunosensor based on versatile carbon nanofibers network coupled with au nanoparticles for aflatoxin B1 detection. Biosensors 2020;11(1):5.

27. Valverde A, Serafín V, Montero CA, Cortes GA, Barderas R, Sedeno YP, *et al*. Carbon/inorganic hybrid nanoarchitectures as carriers for signaling elements in electrochemical immunosensors: First biosensor for the determination of the inflammatory and metastatic processes biomarker rank-ligand. ChemElectroChem 2020;7(3):810-20.
28. Takemura K, Ganganboina AB, Khoris IM, Chowdhury AD, Park EY. Plasmon nanocomposite-enhanced optical and electrochemical signals for sensitive virus detection. ACS Sens 2021;6(7):2605-12.
29. Adabi M, Esnaashari SS, Adabi M. An electrochemical immunosensor based on electrospun carbon nanofiber mat decorated with gold nanoparticles and carbon nanotubes for the detection of breast cancer. J Porous Mater 2021;28(2):415-21.
30. Tao D, Gu Y, Song S, Nguyen EP, Cheng J, Yuan Q, *et al*. Ultrasensitive detection of alpha-synuclein oligomer using a polyD-glucosamine/gold nanoparticle/carbon-based nanomaterials modified electrochemical immunosensor in human plasma. Microchem J 2020;158:105195.
31. Peng J, Zhao Z, Zheng M, Su B, Chen X, Chen X. Electrochemical synthesis of phosphorus and sulfur co-doped graphene quantum dots as efficient electrochemiluminescent immunomarkers for monitoring okadaic acid. Sensor Actuat B-Chem 2020;304:127383.
32. Liu X, Wen Y, Wang W, Zhao Z, Han Y, Tang K, *et al*. Nanobody-based electrochemical competitive immunosensor for the detection of AFB 1 through AFB 1-HCR as signal amplifier. Microchim Acta 2020;187:1-0.
33. Wang Z, Yang S, Wang Y, Feng W, Li B, Jiao J, *et al*. A novel oriented immunosensor based on AuNPs-thionine-CMWCNTs and staphylococcal protein A for interleukin-6 analysis in complicated biological samples. Anal Chim Acta 2020;1140:145-52.
34. He Z, Cai Y, Yang Z, Li P, Lei H, Liu W, *et al*. A dual-signal readout enzyme-free immunosensor based on hybridization chain reaction-assisted formation of copper nanoparticles for the detection of microcystin-LR. Biosens Bioelectron 2019;126:151-9.
35. Hu L, Zheng J, Zhao K, Deng A, Li J. An ultrasensitive electrochemiluminescent immunosensor based on graphene oxide coupled graphite-like carbon nitride and multiwalled carbon nanotubes-gold for the detection of diclofenac. Biosens Bioelectron 2018;101:260-7.
36. Peng C, Ji H, Wang Z. An electrochemical biosensor based on gold nanoparticles/carbon nanotubes hybrid for determination of recombinant human erythropoietin in human blood plasma. Int J Electrochem Sci 2022;17(11):221127.
37. Chen F, Wu Q, Song D, Wang X, Ma P, Sun Y. $Fe_3O_4$@ PDA immune probe-based signal amplification in Surface Plasmon Resonance (SPR) biosensing of human cardiac troponin I. Colloids Surf B Biointerfaces 2019;177:105-11.
38. Maity D, Minitha CR, RT RK. Glucose oxidase immobilized amine terminated multiwall carbon nanotubes/reduced graphene oxide/polyaniline/gold nanoparticles modified screen-printed carbon electrode for highly sensitive amperometric glucose detection. Mater Sci Eng C Mater Biol Appl 2019;105:110075.
39. Wu Q, Li N, Wang Y, Xu Y, Wei S, Wu J, *et al*. A 2D transition metal carbide MXene-based SPR biosensor for ultrasensitive carcinoembryonic antigen detection. Biosens Bioelectron 2019;144:111697.
40. Zhang Q, Fu M, Lu H, Fan X, Wang H, Zhang Y, *et al*. Novel potential and current type chiral amino acids biosensor based on L/D-handed double helix carbon nanotubes@ polypyrrole@ Au nanoparticles@ L/D-cysteine. Sensor Actuat B-Chem 2019;296:126667.
41. Rabai S, Teniou A, Catanante G, Benounis M, Marty JL, Rhouati A. Fabrication of AuNPs/MWCNTS/chitosan nanocomposite for the electrochemical aptasensing of cadmium in water. Sensors 2021;22(1):105.
42. Thu VT, Nga DT, Ly CT, do Chung P, Ngan NT, van Trinh P. Aqueous electrodeposition of (AuNPs/MWCNT-PEDOT) composite for high-affinity acetylcholinesterase electrochemical sensors. J Mater Sci 2020;55(21):9070-81.
43. Du X, Zhang Z, Zheng X, Zhang H, Dong D, Zhang Z, *et al*. An electrochemical biosensor for the detection of epithelial-mesenchymal transition. Nat Commun 2020;11(1):192.
44. Wang Z, Guo H, Gui R, Jin H, Xia J, Zhang F. Simultaneous and selective measurement of dopamine and uric acid using glassy carbon electrodes modified with a complex of gold nanoparticles and multiwall carbon nanotubes. Sensor Actuat B-Chem 2018;255:2069-77.
45. Zhang C, Ren J, Zhou J, Cui M, Li N, Han B, *et al*. Facile fabrication of a 3, 4, 9, 10-perylene tetracarboxylic acid functionalized graphene-multiwalled carbon nanotube-gold nanoparticle nanocomposite for highly sensitive and selective electrochemical detection of dopamine. Analyst 2018;143(13):3075-84.
46. Ibrahim M, Ibrahim H, Almandil N, Kawde AN. Gold nanoparticles/f-MWCNT nanocomposites modified glassy carbon paste electrode as a novel voltammetric sensor for the determination of cyproterone acetate in pharmaceutical and human body fluids. Sensor Actuat B-Chem 2018;274:123-32.
47. Inagaki CS, Oliveira MM, Bergamini MF, Marcolino-Junior LH, Zarbin AJ. Facile synthesis and dopamine sensing application of three component nanocomposite thin films based on polythiophene, gold nanoparticles and carbon nanotubes. J Electroanal Chem 2019;840:208-17.
48. Salvo-Comino C, Rassas I, Minot S, Bessueille F, Arab M, Chevallier V, *et al*. Voltammetric sensor based on molecularly imprinted chitosan-carbon nanotubes decorated with gold nanoparticles nanocomposite deposited on boron-doped diamond electrodes for catechol detection. Materials 2020;13(3):688.
49. Zhang M, Zheng J, Wang J, Xu J, Hayat T, Alharbi NS. Direct electrochemistry of cytochrome c immobilized on one dimensional Au nanoparticles functionalized magnetic N-doped carbon nanotubes and its application for the detection of $H_2O_2$. Sensor Actuat B-Chem 2019;282:85-95.
50. Lotfi S, Veisi H. Synthesis and characterization of novel nanocomposite (MWCNTs/CC-SH/Au) and its use as a modifier for construction of a sensitive sensor for determination of low concentration of levothyroxine in real samples. Chem Phys Lett 2019;716:177-85.
51. Lu Y, Lu X, Gu S, Shi XM, Fan GC. Enhanced two-electrode photoelectrochemical biosensing platform amplified by bilirubin oxidase labelling. Sensor Actuat B-Chem 2021;343:130060.
52. Azadbakht A, Abbasi AR. Impedimetric aptasensor for kanamycin by using carbon nanotubes modified with MoSe2 nanoflowers and gold nanoparticles as signal amplifiers. Microchim Acta 2019;186:1-0.
53. He B, Wang L, Dong X, Yan X, Li M, Yan S, *et al*. Aptamer-based thin film gold electrode modified with

gold nanoparticles and carboxylated multi-walled carbon nanotubes for detecting oxytetracycline in chicken samples. Food Chem 2019;300:125179.

54. Liu X, Deng K, Wang H, Li C, Zhang S, Huang H. Aptamer based ratiometric electrochemical sensing of 17β-estradiol using an electrode modified with gold nanoparticles, thionine, and multiwalled carbon nanotubes. Microchimica Acta 2019;186(6):1-8.
55. Anirudhan TS, Nair SS. Development of voltage gated transdermal drug delivery platform to impose synergistic enhancement in skin permeation using electroporation and gold nanoparticle. Mater Sci Eng C Mater Biol Appl 2019;102:437-46.
56. Karthika V, Kaleeswarran P, Gopinath K, Arumugam A, Govindarajan M, Alharbi NS, *et al*. Biocompatible properties of nano-drug carriers using $TiO_2$-Au embedded on multiwall carbon nanotubes for targeted drug delivery. Mater Sci Eng C Mater Biol Appl 2018;90:589-601.
57. Qin X, Si Y, Wang D, Wu Z, Li J, Yin Y. Nanoconjugates of Ag/Au/carbon nanotube for alkyne-meditated ratiometric SERS imaging of hypoxia in hepatic ischemia. Anal Chem 2019;91(7):4529-36.
58. Saghatchi F, Mohseni-Dargah M, Akbari-Birgani S, Saghatchi S, Kaboudin B. Cancer therapy and imaging through functionalized carbon nanotubes decorated with magnetite and gold nanoparticles as a multimodal tool. Appl Biochem Biotechnol 2020;191:1280-93.
59. Wroblewska A, Gordeev G, Duzynska A, Reich S, Zdrojek M. Doping and plasmonic Raman enhancement in hybrid single walled carbon nanotubes films with embedded gold nanoparticles. Carbon 2021;179:531-40.
60. Cho YM, Lee SS, Park CR, Kim TA, Park M. Enhanced electrical conductivity of polymer microspheres by altering assembly sequence of two different shaped conductive fillers. Compos A Appl Sci Manuf 2021;149:106562.
61. Li Z, Peng J, Lin Z. One-dimensional hairy CNT/polymer/Au nanocomposites *via* ligating with amphiphilic crosslinkable block copolymers. Giant 2021;5:100048.